Sonocatalytic Methylene Blue in The Presence of Fe_3O_4-CuO-TiO_2 Nanocomposites Heterostructure

Malleo Fauzian[1,2], Shofianina Jalaludin[1,2], Ardiansyah Taufik[1,2], Rosari Saleh[1,2,a]
[1]Departemen Fisika, Fakultas MIPA-Universitas Indonesia, 16424 Depok, Indonesia
[2]Integrated Laboratory of Energy and Environment, Fakultas MIPA-Universitas Indonesia, 16424 Depok, Indonesia

[a]Corresponding"s author: rosari.saleh@gmail.com; rosari.saleh@ui.ac.id

Abstract. In this work, the emphasis was mainly placed on investigating the sonocatalytic activity of Fe_3O_4-CuO-TiO_2 nanocomposites heterostructure. The prepared samples were characterized by X-ray diffraction (XRD), Vibrating Sample Magnetometer (VSM), Brunauer-Emmett-Teller (BET) Surface Area Analysis. Methylene blue dye was selected to examine the sonocatalytic activity of Fe_3O_4-CuO-TiO_2 nanocomposites heterostructure. The degradation reaction processes were monitored by UV–vis spectrophotometer. The influence on the activity of the Fe_3O_4-CuO-TiO_2 nanocomposites heterostructure such as TiO_2 loading was studied. The sonocatalyst Fe_3O_4-CuO-TiO_2 with molar ratio of 1:1:5 showed the highest sonocatalytic activity. At last, the experiment also indicated that holes are the main reactive species in the photodegradation mechanism in methylene blue.

1. Introduction

In the recent years, environmental pollution has been found as one of the biggest problem in the rapid growth in the production processes [1]. Therefore, it is required to develop a new and efficient treatment for the removal of a large number of toxic compounds in the effluents discharged from the industry. As one of advanced oxidation technology, the sonocatalytic degradation has gain more attention for purification of polluted effluents and has good prospect for protecting the environment [2-4]. However, degradation of toxic complex compounds using ultrasound consumes large amounts of energy if one applying sonolysis alone [5]. Therefore, ultrasonic wastewater treatment can be performed in the presence of catalyst. Heterostucture catalysts have received immense interest since they offer a great potential to solve problem of environmental pollution and energy crisis [6]. Among the various heterostructure catalyst, TiO_2−CuO nanocomposites heterostructure is one of the promising materials. Recently, there have been reports of materials having both adsorption and oxidation properties, that are important in degradation of polluted effluents. Fe_3O_4 has been found to possess ferromagnetic behavior, and it can be used as an adsorbent with a large area and small diffusion resistance for removal of chemical species such as organic pollutants [7-9].

The present study aims to investigate the Fe_3O_4-CuO-TiO_2 mediated sonocatalytic degradation of methylene blue as a model of the toxic complex compounds because of its complex aromatic ring structure is difficult to remove from the environtment [10]. The influence of different TiO_2 loading of Fe_3O_4-CuO-TiO_2 nanocomposites heterostructure in the aqueous solution on the sonocatalytic efficiency was evaluated. The presence of radical scavangers was employed to provide insight on the photo-degradation mechanism through different active species.

2. Experimental

A series of Fe_3O_4-CuO-TiO_2 nanocomposites nanoparticles were prepared using sol-gel method described previously with the variation of molar ratio of 1:1:1, 1:1:3 and 1:1:5 [11-13].

The structure and phase of the samples were characterized by X-ray diffraction (XRD) measurements using a Philips PW 1710. Magnetic measurements were performed on Oxford type 1.2 T vibrating sample magnetometer (VSM). The nitrogen ad/desorption isotherms were measured using Nova Quantachrome 2000.

Sonocatalytic activity was evaluated by degradation of Methylene blue (MB) in the presence of Fe_3O_4-CuO-TiO_2 nanocomposite in aqueous solutions using ultrasonic bath operated at fixed frequency of 40 kHz. In the experiment, typically 20 mg Fe_3O_4-CuO-TiO_2 nanocomposite catalyst was suspended in 100 mL MB solution with 20 mg/L concentration of MB. The suspended solution was placed in the dark for 30 min under magnetic stirring to ensure the establishment of an adsorption-desorption equilibrium in MB solution. After that period of time, the ultrasonic bath was turned on and this was taken as 'time zero" for the reaction. During the sonocatalytic reaction, samples were collected for 2 h at regular intervals. The solution was analyzed using a Dynamica UV-visible spectrophotometer with a quartz cuvette with an optical length of 10 mm.

3. Results and discussion

The influence of ultrasonic irradiation on MB degradation by Fe_3O_4-CuO-TiO_2 nanocomposites were investigated and plotted in Figure 1a. The ability of ultrasound to degrade MB in the presence of Fe_3O_4-CuO-TiO_2 nanocomposites with various TiO_2 loading was compared. It is seen, that Fe_3O_4-CuO-TiO_2 nanocomposites with molar ratio of 1:1:5 has degraded the most of MB (92%), whereas nanocomposites with molar ratio of 1:1:1 and 1:1:3 degraded 83 % and 87% of MB, respectively. The sonocatalytic activity of all samples in this study obeys the pseudo-first-order reaction kinetics [5, 8]. The apparent reaction rate constant *k* of the MB degradation using three different molar ratio of Fe_3O_4-CuO-TiO_2 nanocomposites are plotted in the inset of Figure 2a. It is clear that the degradation efficiency increases with the increase in TiO_2 loading in our nanocomposites.

To get insight of the degradation mechanism, control experiments have been carried out by adding different type of scavengers. The degradation of MB in the presence of tert-butyl alcohol, ammonium oxalate and $Na_2S_2O_8$ scavenger for hydroxyl radicals, holes and electrons, respectively, is displayed in Figure 2b. It is obvious that the order of affecting the rate for degradation of MB follows that of hole > hydroxyl radical > electron. It can be seen that ammonium oxalate provoke a large degree of inhibition

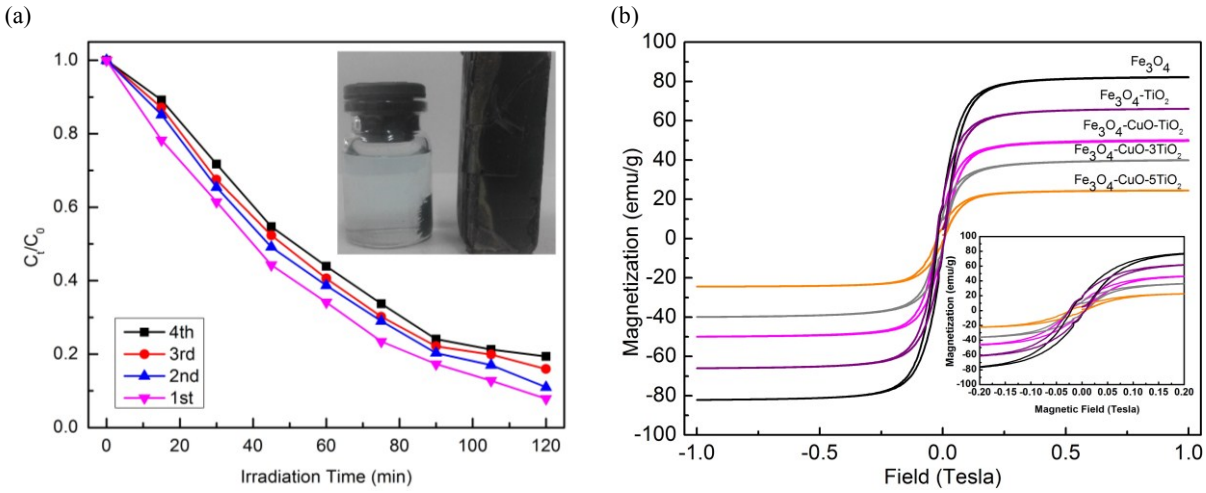

Figure 1. (a) Reusability of Nanocomposites, (b) VSM spectra of Fe_3O_4 and Fe_3O_4-CuO-TiO_2 [13].

Table 1. Magnetic Properties, Grain Size, and Surface Area Analysis.

Sample	M-S (emu/g)	Hc (Tesla)	mr (emu/g)	Grain Size (nm) Fe_3O_4	Grain Size (nm) CuO	Grain Size (nm) TiO_2	Surface Area (m^2/g)	Pore Size (nm)	Pore volume (cc/g)
Fe_3O_4	82	0.0152	13.64	45	-	-	-	-	-
CuO	-	-	-	-	15	-	-	-	-
TiO_2	-	-	-	-	-	33	-	-	-
Fe_3O_4-TiO_2	66	0.0149	12.91	44	-	64	-	-	-
Fe_3O_4-CuO-TiO_2	50	0.0151	7.79	42	18	53	18.36	1.51	0.04
Fe_3O_4-CuO-3TiO_2	40	0.015	6.49	39	24	70	27.12	3.04	0.08
Fe_3O_4-CuO-5TiO_2	25	0.0149	3.66	45	35	84	37.64	1.02	0.16

of MB, which confirmed the indispensable role of holes in the degradation process of MB. Thus, a lower percentage of degradation of MB was obtained, suggesting that the sonocatalytic activity of MB is driven by holes.

It is known that reusability and stability of catalysts are important parameters of the degradation process and are important issues for practical applications. To evaluate the stability of the catalyst

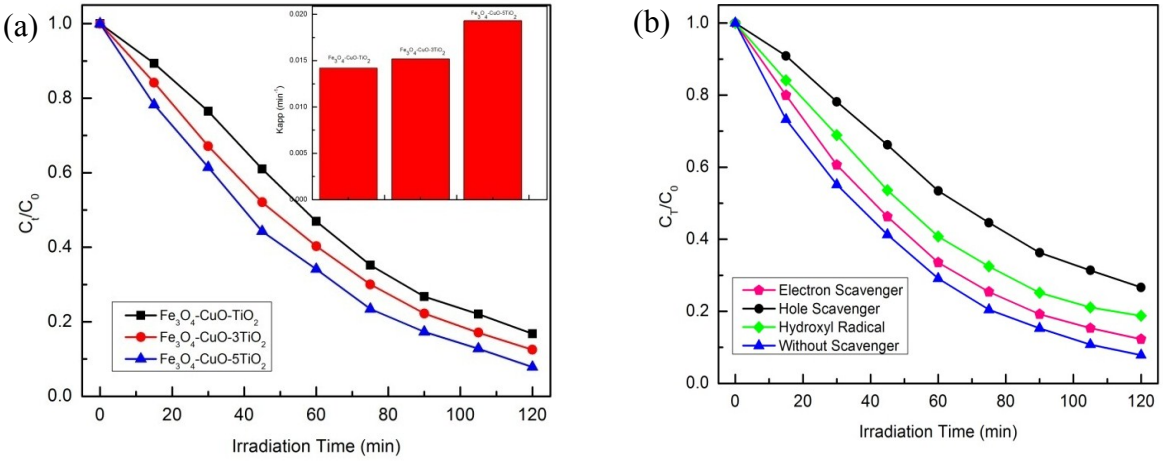

Figure 2. (a) Sonocatalytic activity of Fe_3O_4-CuO-TiO_2 nanocomposites with various molar ratio, (b) Effect of scavenger on sonocatalytic activity of Fe_3O_4-CuO-5TiO_2.

under ultrasonic irradiation, the Fe_3O_4-CuO-TiO_2 nanocomposites with a molar ratio of 1:1:5 were repeatedly used for four cycles. In this experiment, nanocomposites could be easily recovered from the solution using a permanent bar magnet (the inset of Figure 1a). The stability was evaluated by reusing the catalyst with the same quantity of fresh MB. The results displayed in Figure. 1a. It is seen, that after four cycles degradation efficiencies of 80% was obtained.

Figure 1b illustrates the magnetic hysteresis curves of Fe_3O_4 nanoparticles, Fe_3O_4-TiO_2 nanocomposites and Fe_3O_4-CuO-TiO_2 nanocomposites recorded at room temperature. The curve of Fe_3O_4-TiO_2 is also shown in the Figure 1b. The coercivity (Hc), magnetic saturation (M-S) and magnetic remanent (mr) are listed in Table 1. The saturation magnetization decreases gradually with incorporation of TiO_2 nanoparticles and decreased further as CuO incorporated into Fe_3O_4-TiO_2 nanocomposites. The reduction of strength of the super exchange interaction among Fe^{3+} ions with incorporation of diamagnetic TiO_2 in Fe_3O_4-TiO_2 and anti-ferromagnetic CuO in Fe_3O_4-CuO-TiO_2 nanocomposites are responsible for the observed reduction of saturation magnetization [14]. However, the saturation magnetization of Fe_3O_4-CuO-TiO_2 nanocomposites is still large enough for magnetic separation as can be seen in the inset of Figure 2a.

Phase composition and crystallite size of samples are reported to have influence on the sonocatalytic activity. Therefore, XRD measurements are conducted in this study. XRD patterns of nanocomposite Fe_3O_4-CuO-TiO_2 are shown in Figure 3. The characteristic diffraction peaks of all nanocomposites samples clearly identified as individual crystal structure and phase of cubic spinel Fe_3O_4, anatase TiO_2 and monoclinic CuO. Additionally, no diffraction peaks assignable to other segregation of phase was observed in the XRD pattern. The crystallite size calculated according to the Scherrer equation [15-16] and unit cell parameters of all samples are tabulated in Table 1.

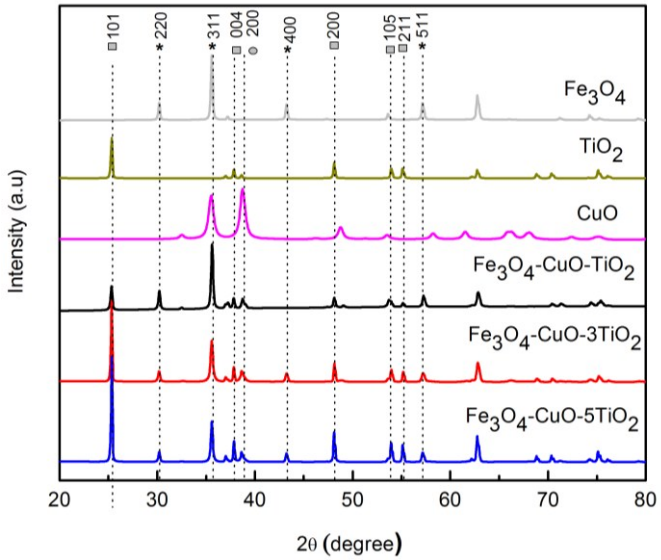

Figure 3. XRD Pattern of Fe_3O_4, CuO, and TiO_2 nanoparticles and Fe_3O_4-CuO-TiO_2 with various molar ratio [13].

The nitrogen adsorption-desorption isotherms of nanocomposites are exhibited in Figure 4. It can be seen clearly in the figure that all samples exhibited a typical type III isotherm with a distinct H3 hysteresis loop according to the IUPAC classification. Table 1 also shows a comparison of the BET surface area, pore volume and pore diameter of all nanocomposite samples were listed in Table 1. This observation suggests that the BET surface area is significantly improved by increasing molar ratio of nanocomposites from 1:1:1 to 1:1:5. It can be seen from the table that the nanocomposite with Fe_3O_4-CuO-TiO_2 molar ratio of 1:1:5 shows a larger specific BET surface area of approximately 37.64 m^2/g. Moreover, the average pore size of Fe_3O_4-CuO-TiO_2 nanocomposites were calculated from desorption branches of the N_2 isotherms via the BJH method.

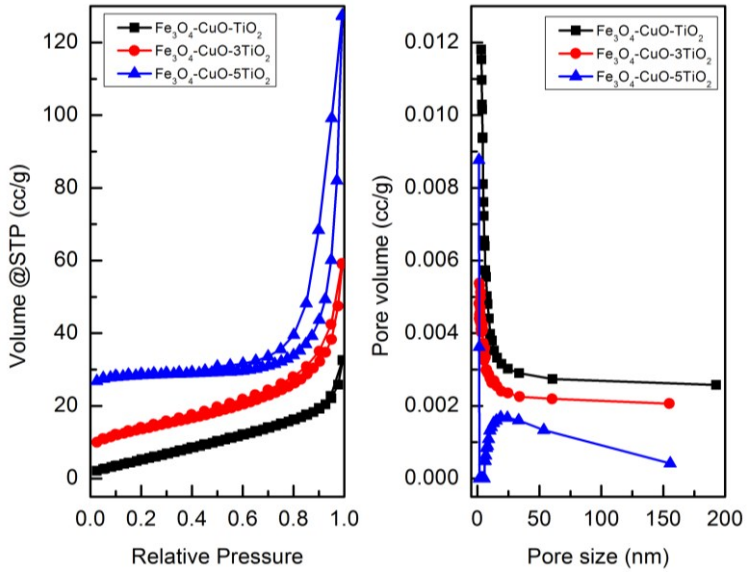

Figure 4. Nitrogen adsorpsion desorpsion and pore size distribution of Fe_3O_4-CuO-TiO_2 with various molar ratio.

It is believed that ultrasonic irradiation can result in the formation of light with comparative band gap energy that could excite electron from valence to conduction band, leaving behind holes in the valence band [17]. Although there have not been satisfying explanation on the sonocatalytic degradation of organic dyes, but the mechanism is often related to the two points of view, namely phenomena of sonoluminescence and "hot spot" [18]. The key steps involved in the mechanism of heterogeneous photocatalyst are charge-carrier generation, charge-carrier trapping, charge-carrier recombination and photocatalytic degradation of organic dye [19]. Moreover there are several parameters that control the photocatalytic activity such as phase purity [20], average crystallite size [21], band gap [22], specific surface area [23] and defect or localized states [24]. It is observed from BET measurements an increase in the specific surface area with increasing TiO_2 loading. However, according to the XRD measurements, the crystallite size did not change significantly. The BET surface areas of samples with molar ratios of 1:1:1 and 1:1:5 are 18.36 and 37.64 cm^2/g, respectively. It has been reported that an increase in the specific surface area will increase the surface active site, which consequently leads to a higher interfacial charge carrier transfer for catalysis, and will enhance the catalytic activity.

It is also reported that the presence of defects or trapping states in catalysts promote the catalytic activity, since defects can act as charge carrier traps for generated electrons and holes under irradiation and can enhance the charge separation, which in turn restrains the loss due to charge recombination. From ESR studies (Figure 5) in our samples confirmed the presence of different kinds of trapping states such as Fe^{3+}, Fe^{2+}, Oxygen vacancy and Cu^{2+} as can be seen in Table 2 [25-28]. It has been reported [26], that these states could trap the generated electrons and later react with the adsorbed O_2 molecules to yield O_2^-. Holes not only could directly decompose the adsorbed dye molecules on the

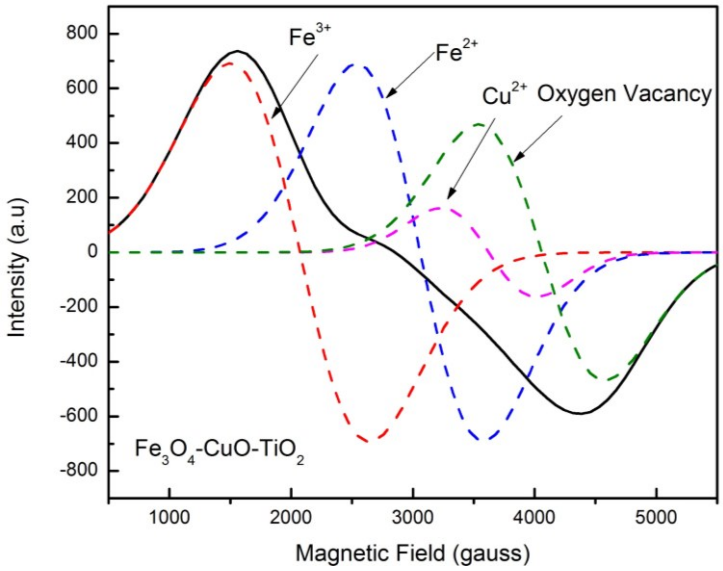

Figure 5. ESR Signal Fe_3O_4-CuO-TiO_2 nanocomposites.

Table 2. ESR Signal Analysis.

Sample	g value	Δ Hpp	Analytical Area	Assign to
Fe_3O_4-CuO-TiO_2	4.50	1141.993	9.33 x 10^8	Fe^{3+}
	2.66	1039.858	7.72 x 10^8	Fe^{2+}
	2.09	779.858	1.02 x 10^8	Cu^{2+}
	2.03	1036.574	5.20 x 10^8	Oxygen Vacancy

surface of the catalyst, it could also accelerate the generation of OH radicals through oxidizing water molecules in the bulk solution. In addition, the "hot spot" produced by ultrasonic cavitation in water medium can produce high temperature that is sufficiently brings about the many holes producing OH radicals on the surface of catalyst. As the molar ratio increased, the probability of electrons collecting in the trapping state increased due to the increase in Ti^{4+}, and more holes can react with the hydroxyl group. Thus, it is concluded that holes play the most important role in the degradation of MB, which is in agreement with the results of experiments using scavenger technique, as shown in Figure 1b.

4. Conclusion

In summary, the present study shows that MB as an organic dye can be removed using ultrasonic irradiation in the presence of Fe_3O_4-CuO-TiO_2 nanocomposites heterostructure. The sonocatalytic activity increased with increasing TiO_2 loading (molar ratio). This might be due to the higher surface area and the enhancement of electron-hole separation. The scavengers such as tert-butyl alcohol, ammonium oxalate and $Na_2S_2O_8$ reduced the MB degradation. Among them, ammonium oxalate was the most effective. These results indicated that holes play an important role in the degradation mechanism of MB.

References

[1] V. M. Correia, T. Stephenson, S.J. Judd, Environmental Technology 15 (1994) 917–924.
[2] E. Sayan, M.E. Edecan, Ultrasonic Sonochememistry 15 (2008) 530–538.
[3] M. Mrowetz, C. Pirola, E. Selli, Ultrasonic Sonochemistry 10 (2003) 247–254.
[4] A. Wang, W. Guo, F. Hao, X. Yue, Y. Leng, Ultrasonic Sonochemistry 21 (2014) 572–575.
[5] J. Wang, Z. Jiang, Z. Zhang, Y. Xie, Y. Lv, J. Li, Y. Deng, X. Zhang, Separation and Purification Technology 67 (2009) 38–43.
[6] B. Li , L. Li , K. Lin , W. Zhang , S.Lu, Q.Luo, Ultrasonics Sonochemistry 20 (2013) 855–863.
[7] N. A. Jamalluddin, A.Z. Abdullah, Ultrasonics Sonochemistry 18 (2011) 669–678.
[8] S. N. R. Inturi, T.Boningari, M. Suidanb, P.G. Smirniotis, Applied Catalysis B: Environmental 144 (2014) 333–342.
[9] A. Z. Abdullah, P.Y. Ling, Journal of Hazardous Materials 173 (2010) 159–167.
[10] Y. Xia, Q. Yao, W. Zhang, Y. Zhang, M. Zhao, Arabian Journal of Chemistry doi:10.1016/j.arabjc.2015.03.010
[11] Z. Xi, C. Li, L. Zhang, M. Xing, J. Zhang, International Journal of Hydrogen Energy 39 (2014) 6345-6353.
[12] S. A. Arifin, S.D.A Jalaludin, R. Saleh, Advanced Materials Research 1123 (2015) 264-269.
[13] S. A. Arifin, S.D.A Jalaludin, R. Saleh, Materials Science Forum 827 (2015) 49-55.
[14] S. D. A Jalaludin, S.A. Arifin, R. Saleh, Materials Science Forum 827 (2015) 13-18.
[15] R.Y. Hong, S.Z. Zhang, G.Q. Di, H.Z. Li, Y. Zheng, J. Ding, D, G. Wei, Preparation, Materials Research Bulletin 43 (2008) 2457-2468.
[16] A. Hamrouni, H. Lachheb, A. Houas, Materials Science and Engineering B 178 (2013) 1371-1379.
[17] A. Cai, Y. Sun, L. Du, X. Wang, Journal of Alloys and Compounds 644 (2015) 344-340.
[18] Y. L. Pang, A. Z. Abdullah, Chemical Engineering Journal 214 (2013) 129–138.
[19] J. Xia, A. Wang, X. Liu, Z. Su, Applied Surface Science 257 (2011) 9724-9732.
[20] C. Hariharan , Applied Catalysis A: General 304 (2006) 55-61.
[21] S. Mukhopadhyay, P. P. Das, S. Maity, P. Ghosh, P.S. Devi, Applied Catalysis B: Environmental 165 (2015) 128-138.
[22] H. Liu, T. Lv, C. Zhu, X. Su, Z. Zhu, Journal of Molecular Catalysis A: Chemical, 396 (2015) 136-142.

[23] J. Huang, S. Wen, J. Liu, G. He, Journal of Natural Gas Chemistry 21 (2012) 302-307.
[24] G. Plantard, V. Goetz, Chemical Engineering Journal 252 (2014) 194-201.
[25] L. Li, H.W. Tian, F. L. Meng, X. Y. Hu, W. T Zheng, C. Q. Sun, Applied Surface Science 317 (2014) 568-572.
[26] A.V. Kucherov, D. E. Doronkin, A.Y. Stakheev, A. L. Kustov, M. Grill, Journal of Molecular Catalysis A: Chemical 325 (2010) 73–78.
[27] J. Zhang, Z. Jin, C.Feng, L. Yu, J Zhang, Z. Zhang, Journal of Solid State Chemistry 184 (2011) 3066-3073.
[28] J. M. Coronado, J. Soria, Catalyst Today 123 (2007) 37-41.